

SYNCHRONIZATION IN NETWORK OF PIERCE DIODES

Anastasiya Filatova

Faculty of Nonlinear Processes
Saratov State University
Russia
rabbit@nonlin.sgu.ru

Alexander Hramov

Faculty of Nonlinear Processes
Saratov State University
Russia
aeh@nonlin.sgu.ru

Alexey Koronovskii

Faculty of Nonlinear Processes
Saratov State University
Russia
alkor@nonlin.sgu.ru

Stefano Boccaletti

CNR — Istituto dei Sistemi Complessi
Via Madonna del Piano
Italy
The Italian Embassy in Tel Aviv
Israel
stefano.boccaletti@fi.isc.cnr.it

Abstract

We report results on synchronization processes in complex networks of spatially extended chaotic systems. The method of the analysis of the stability of the network synchronous spatio-temporal state has been developed. The technique both for the stability analysis of the synchronous state in such systems and for the spatial master stability function calculation has been developed. The efficiency of the proposed approach has been illustrated by the consideration of the complex network of beam-plasma chaotic systems (Pierce diodes).

Key words

synchronization, network, spatially extended chaotic systems

Introduction

The sophisticated collaborative dynamics of interacting elements described by means of complex networks become the objects of interest for the broad scientific community (see (Boccaletti S., Latora V., Moreno V., Chavez M., Hwang D.-U., 2006) and references therein). Complex networks are objects characterized by a path-length ℓ scaling logarithmically with the network size N ($\ell \propto \log N$, in contrast to the linear scaling of regular lattices), but yet a clustering structure much more prominent than that characterizing a random graph.

Recently, the dynamics of complex networks has been extensively investigated with regard to collective (synchronized) behaviors (Boccaletti S., Kurths J., Osipov G., Valladares D.L., Zhou C.S., 2002), with special

emphasis on the interplay between complexity in the overall topology and local dynamical properties of the coupled units. The usual case considered so far is that of networks of identical dynamical systems coupled by means of a complex wiring of connections. In this framework, several studies have shown how to enhance synchronization properties, by properly weighting the strengths of the connection wiring (Chavez M., Hwang D.-U., Amann A., Hentschel H.G.E., Boccaletti S., 2005; Hwang D.-U., Chavez M., Amann A., Boccaletti S., 2005; Motter A.E., Zhou C., Kurths J., 2005; Zhou C., Motter A.E., Kurths J., 2006; Motter A.E., Zhou C.S., Kurths J., 2005).

At the same time, the majority of works devoted to complex network synchronization deal with the node elements characterized by the small number of degrees of freedom (Dorogovtsev S.N., Mendes J.F.F., 2003; Albert R., Barabási A.L., 2002; Watts D.J., 1999; Watts D. J., Strogatz S., 1998; Belykh I., Belykh V., Hasler M., 2004). In this paper we extend the study of synchronization phenomena in complex networks to the case of spatially extended coupled dynamical systems, i.e. networks whose nodes are represented by dynamical systems each one of them is described by partial differential equations. This is motivated by the fact that such a representation seems to be a more adequate description of many relevant phenomena occurring in natural systems. The study of such networks allows to understand better the fundamental aspects of chaotic synchronization including transition between different types of synchronous dynamics as well as interrelation between synchronization of spatially extended systems and synchronization of the systems with the small number of degree of freedom.

The consideration of the networks whose nodes are represented by the microwave beam-plasma systems is also of interest in connection with the nonlinear antenna technology (Ito H., Mosekilde E. et al., 1993; Ditto W. L., Spano M. L. et al., 1995; Meadows B.K., Heath T.H. et al., 2002). Indeed, the studies of the synchronous state stability of the active nonlinear antenna module were carried out (Ito H., Mosekilde E. et al., 1993; Ditto W. L., Spano M. L. et al., 1995; Meadows B.K., Heath T.H. et al., 2002), with the elements being the nonlinear systems with the small number of degree of freedom (the radio technical generators have been considered as the components of the nonlinear antenna). Nevertheless, the use of the spatially extended high-power microwave devices (such as backward wave oscillators (Bezruchko B.P., Kuznetsov S.P., Trubetskov D.I., 1979; Ginzburg N.S., Kuznetsov S.P., Fedoseeva T.N., 1979; Levush B., Antonsen T.M., Bromborsky A., Lou W.R., Carmel Y., 1992), Pierce diodes (Godfrey B.B., 1987; Matsumoto H., Yokoyama H., Summers D., 1996; Klinger T., Schroder C., Block D., Greiner F., Piel A., Bonhomme G., Naulin V., 2001), klystron generators (Shigaev A.M., Dmitriev B.S., Zharkov Yu.D.; Ryskin N.M., 2005), gyro-devices (Felch K.L., Danly B.G., Jory H.R. et al, 1999; Nusinovich G.S., Vlasov A.N., Antonsen T.M., 2001), etc.) as pieces of the nonlinear antenna is more appropriate for the practical purpose.

So, the consideration of the synchronous dynamics of the network of the spatially extended systems used as the node elements proves to be of importance. In our paper such a spatially extended microwave beam-plasma object as Pierce diode has been selected as node element, although the developed formalism may be easily used to analyze the stability of the synchronous state of the network with the different extended systems. It is important to note that the Pierce diode is the well studied model of the beam-plasma systems demonstrating the complex chaotic oscillations. In particular, the routes to the spatial chaos (Godfrey B.B., 1987; Matsumoto H., Yokoyama H., Summers D., 1996), pattern formation (Kuhn S., Ender A., 1990; Kolinsky and Schamel, 1995), controlling chaos (Friedel H., Grauer R., Spatschek H.K., 1998; Klinger T., Schroder C., Block D., Greiner F., Piel A., Bonhomme G., Naulin V., 2001; Hramov A.E., Rempen I.S., 2004; Hramov A.E., Koronovskii A.A., Rempen I.S., 2006) and synchronization (Hur M.S., 1998; Filatov R.A., Hramov A.A., Koronovskii A.A., 2006) have been studied in detail for Pierce diode.

1 Pierce diode

Pierce diode (Pierce J.R., 1944; Godfrey B.B., 1987; Matsumoto H., Yokoyama H., Summers D., 1996) is one of the simple spatially extended microwave beam-plasma systems in which the complicated chaotic dynamics have been observed (Godfrey B.B., 1987; Kuhn S., Ender A., 1990; Lindsay P.A., Chen X.,

Xu M., 1995; Matsumoto H., Yokoyama H., Summers D., 1996; Klinger T., Latten A., Piel A., Bonhomme E., Pierre T., 1997; Hramov A.E., Rempen I.S., 2004). It consists of two infinite parallel plains pierced by a mono-energetic electron beam (Fig. 1). Grids are grounded, with the distance between them being L . The charge density ρ_0 and electron velocity v_0 are constant at the system input. The region between two plains is uniformly filled by neutralizing stationary ions, with density $|\rho_i|$ being equal to the non-perturbed electron beam density $|\rho_0|$.

The dimensionless Pierce parameter $\alpha = \omega_p L / v_0$ determines the dynamics of the system (here ω_p is the electron beam plasma frequency, v_0 is the non-perturbed electron velocity, L is the distance between the diode plains). With $\alpha > \pi$, the so-called Pierce instability develops in the system and the virtual cathode is formed in the electron beam (Pierce J.R., 1944; Matsumoto H., Yokoyama H., Summers D., 1996). At the same time in a narrow range of Pierce parameter values near $\alpha \sim 3\pi$ the increase of the instability is suppressed by the non-linearity and the regime without reflection takes place in the electron beam (Matsumoto H., Yokoyama H., Summers D., 1996; Trubetskov A.E., Hramov A.E., 2003). In this case the system behavior may be described by the fluid equations (Trubetskov A.E., Hramov A.E., 2003; Godfrey B.B., 1987; Matsumoto H., Yokoyama H., Summers D., 1996). It is known (Godfrey B.B., 1987; Kuhn S., Ender A., 1990; Lindsay P.A., Chen X., Xu M., 1995; Matsumoto H., Yokoyama H., Summers D., 1996; Hramov A.E., Rempen I.S., 2004) that various types of beam-plasma chaotic oscillations may be observed in this regime.

The behavior of Pierce diode in the fluid electronic approximation is described by the self-congruent system of dimensionless Poisson, continuity and motion equations

$$\frac{\partial^2 \varphi}{\partial x^2} = \alpha^2 (\rho - 1), \quad (1)$$

$$\frac{\partial \rho}{\partial t} = -\frac{\partial(\rho v)}{\partial x}, \quad (2)$$

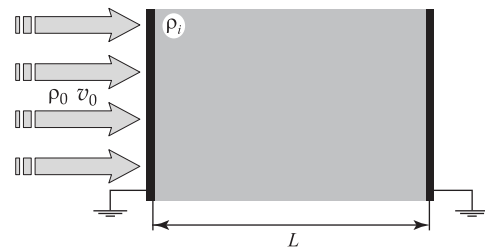


Figure 1. Schematic diagram of Pierce diode

$$\frac{\partial v}{\partial t} = -v \frac{\partial v}{\partial x} - \frac{\partial \varphi}{\partial x}, \quad (3)$$

with the boundary conditions:

$$\varphi(0, t) = \varphi(1, t) = 0, \quad \rho(0, t) = 1, \quad v(0, t) = 1, \quad (4)$$

where $\varphi(x, t)$ is the dimensionless potential of the electric field ($0 \leq x \leq 1$), $\rho(x, t)$ and $v(x, t)$ are the dimensionless density and velocity of the electron beam, respectively. The dimensional variables (φ' , ρ' , v' , x' , t') are connected with the dimensionless ones as

$$\varphi' = (v_0^2/\eta)\varphi, \quad \rho' = \rho_0\rho,$$

$$v' = v_0v, \quad x' = Lx, \quad t' = (L/v_0)t, \quad (5)$$

where η is the specific electron charge, v_0 and ρ_0 are the non-perturbed velocity and density of the electron beam.

The behavior of two Pierce diodes coupled both unidirectionally and mutually has been considered in (Filatov R.A., Hramov A.A., Koronovskii A.A., 2006), with the coupling between systems being realized by the modulation of the dimensionless potential value on the right bound of the systems (see (Filatov R.A., Hramov A.A., Koronovskii A.A., 2006; Hramov A.E., Koronovskii A.A., Popov P.V., Rempen I.S., 2005) for detail). The synchronization of the external harmonic signal (Hur M.S., 1998) and the different types of chaotic synchronization (i.e., time scale synchronization (Hramov A.E., Koronovskii A.A., 2004; Hramov A.E., Koronovskii A.A., 2005b), generalized synchronization (Rulkov N.F., Sushchik M.M., Tsimring L.S., Abarbanel H.D.I., 1995; Abarbanel H.D.I., Rulkov N.F., Sushchik M.M., 1996; Hramov A.E., Koronovskii A.A., 2005a; Hramov A.E., Koronovskii A.A., Popov P.V., 2005), lag-synchronization (Rosenblum M.G., Pikovsky A.S., Kurths J., 1997; Taherion S., Lai Y.C., 1999) and complete synchronization (Pecora L.M., Carroll T.L., 1990; Pecora L.M., Carroll T.L., 1991)) have been observed for the considered system (Filatov R.A., Hramov A.A., Koronovskii A.A., 2006). Therefore, it seems to be likely that the network consisting of Pierce diodes may show the synchronous dynamics under the certain conditions, if the diodes are coupled in the same way, i.e., by the modulation of the potential value on the right bound of each system. The detailed description of such a network as well as the method of the analysis of the synchronous state stability are given in the next section.

2 Stability of the synchronous state of complex network consisting of spatially extended systems

Let us consider the network of N Pierce diodes used as the node elements. The behavior of the

i -th node of the network is described by the state $\mathbf{U}_i(x, t) = (\varphi_i(x, t), \rho_i(x, t), v_i(x, t))^T$, with the dimensionless potential $\varphi_i(x, t)$ of the electric field, density $\rho_i(x, t)$ and velocity $v_i(x, t)$ of the electron beam being described by equations (1)–(3). Let us denote the evolution operator (1)–(3) of the i -th node as

$$\hat{L}(\mathbf{U}_i) = 0. \quad (6)$$

The influence of links between nodes of the network results in the variation of the potential value $\varphi_i(1, t)$ on the right boundary of i -th Pierce diode (see (Filatov R.A., Hramov A.A., Koronovskii A.A., 2006; Hramov A.E., Koronovskii A.A., Popov P.V., Rempen I.S., 2005) for detail) according to the states of the another node elements

$$\varphi_i(1, t) = -\sigma \sum_{j=1}^N G_{ij} \rho_j(1, t), \quad (7)$$

where σ is the coupling strength of links between nodes, $\rho_j(1, t)$ is the dimensionless electron beam density in the point with the coordinate $x = 1$ corresponding to the output grid of j -th Pierce diode. G is the Laplacian matrix of the network. As so, it is a symmetric zero row sum matrix, it has a real spectrum of eigenvalues $\lambda_1 \geq \dots \geq \lambda_N$, G_{ij} ($i \neq j$) is equal to 1 whenever node i is connected with node j and 0 otherwise, and $G_{ii} = -\sum_{j \neq i} G_{ij}$.

If the network elements demonstrate the complete synchronization regime the states of all Pierce diodes coincide with each other $\mathbf{U}_i(x, t) = \mathbf{U}_s(x, t), \forall i$, with the boundary condition (7) taking the form $\varphi_i(1, t) = \varphi_s(1, t) = 0, \forall i$. One can see that the interaction between the node elements of the network is vanishingly small for the complete synchronization regime.

With the small perturbation $\xi = (\xi^\varphi, \xi^\rho, \xi^v)^T$ of the synchronous state \mathbf{U}_s existing, the behavior of the i -th node of the network is described by equation

$$\hat{L}(\mathbf{U}_s + \xi_i) = 0 \quad (8)$$

with the boundary conditions

$$\begin{aligned} \varphi_i(1, t) + \xi_i^\varphi(1, t) &= -\sigma \sum_{j=1}^N G_{ij} (\rho_j(1, t) + \xi_j^\rho(1, t)), \\ \rho_i(0, t) + \xi_i^\rho(0, t) &= 1, \\ v_i(0, t) + \xi_i^v(0, t) &= 1. \end{aligned} \quad (9)$$

Taking into account the vanishingly small values of the perturbations of the synchronous state \mathbf{U}_s the evolution operator (6) may be rewritten as

$$\partial \hat{L}(\mathbf{U}_s, \xi_i) = 0, \quad (10)$$

where $\partial\hat{L}(\mathbf{U}_s, \xi_i)$ is the linearization of the evolution operator $\hat{L}(\cdot)$ in the vicinity of the synchronous state $\mathbf{U}_s(x, t)$, therefore, it is linear for the perturbation $\xi(x, t)$. For the considered Pierce diode model the linearized operator $\partial\hat{L}(\mathbf{U}_s, \xi)$ is

$$\begin{aligned}\frac{\partial^2 \xi^\varphi}{\partial x^2} &= \alpha^2 \xi^\rho, \\ \frac{\partial \xi^\rho}{\partial t} &= -\xi^\rho \frac{\partial v_s}{\partial x} - v_s \frac{\partial \xi^\rho}{\partial x} - \xi^v \frac{\partial \rho_s}{\partial x} - \rho_s \frac{\partial \xi^v}{\partial x}, \quad (11) \\ \frac{\partial \xi^v}{\partial t} &= -v_s \frac{\partial \xi^v}{\partial x} - \xi^v \frac{\partial v_s}{\partial x} - \frac{\partial \xi^\varphi}{\partial x}\end{aligned}$$

According to (4) and (9) the boundary conditions for the perturbation ξ_i take the form

$$\begin{aligned}\xi_i^\varphi(1, t) &= -\sigma \sum_{j=1}^N G_{ij} \xi_j^\rho(1, t), \\ \xi_i^\rho(0, t) &= 0, \\ \xi_i^v(0, t) &= 0.\end{aligned}\quad (12)$$

Obviously, the matrix G determining the structure of the links between nodes of the network may be transformed to the diagonal form

$$\tilde{\mathbf{G}} = \begin{pmatrix} \lambda_1 & 0 & \dots & 0 \\ 0 & \lambda_2 & \dots & 0 \\ \vdots & \vdots & \ddots & \vdots \\ 0 & 0 & \dots & \lambda_N \end{pmatrix}, \quad (13)$$

and the stability of the synchronous state $[\mathbf{U}_i(x, t) = \mathbf{U}_s(x, t), \forall i]$ is determined by the N evolution operators

$$\partial\hat{L}(\mathbf{U}_s, \varsigma_i) = 0 \quad (14)$$

with the boundary conditions

$$\begin{aligned}\varsigma_i^\varphi(1, t) &= -\sigma \lambda_i \varsigma_i^\rho(1, t), \\ \varsigma_i^\rho(0, t) &= 0, \\ \varsigma_i^v(0, t) &= 0.\end{aligned}\quad (15)$$

Equations (14) and (15) differ from each other only by the eigenvalues $\lambda_1 \geq \dots \geq \lambda_N$ of the coupling matrix G .

The synchronous state $[\mathbf{U}_i(x, t) = \mathbf{U}_s(x, t), \forall i]$ is stable if all perturbations ς_i decrease. For the system with the small number of degrees of freedom the stability of the synchronous state of the network may be analyzed by means of the largest Lyapunov exponent [also called master stability function (Pecora L.M., Carroll T.L., 1998)]. In this paper (see Sec. 3) we propose the quantity allowing to characterize the stability of the spatially extended system called as *spatial*

master stability function (SMSF). As it will be shown below SMSF is similar to the largest Lyapunov exponent in the system with the small number of degrees of freedom. Replacing $(-\sigma \lambda_i)$ by ν in equation (15), the behavior of SMSF Λ vs ν completely accounts for the linear stability of the synchronized state. Indeed, the synchronized state associated with $\lambda_1 = 0$ is stable when all the remaining equations (14) with the boundary conditions (15) related with the other eigenvalues λ_i ($i = 2, \dots, N$) of the coupling matrix G are characterized by the negative SMSF. So, to analyze the stability of the synchronized state $\mathbf{U}_s(x, t)$ of the network only one equation

$$\partial\hat{L}(\mathbf{U}_s, \varsigma) = 0 \quad (16)$$

from (14) with the parametric boundary conditions

$$\begin{aligned}\varsigma^\varphi(1, t) &= \nu \varsigma_i^\rho(1, t), \\ \varsigma^\rho(0, t) &= 0, \\ \varsigma^v(0, t) &= 0.\end{aligned}\quad (17)$$

should be considered to obtain the dependence of the SMSF Λ on the parameter ν . Furthermore, the synchronous state $\mathbf{U}_s(x, t)$ may be obtained as a solution of the evolution equation (6) with the boundary conditions (4).

It seems likely that SMSF $\Lambda(\nu)$ may be negative for a finite interval of ν -parameter values $I_{st} = (\nu_1; \nu_2)$ or for an infinite one ($\nu_2 = \infty$) just as the largest Lyapunov exponent does in (Pecora L.M., Carroll T.L., 1998). The stability condition is satisfied if the whole set of eigenvalues λ_i ($i = 2, \dots, N$) multiplied by the same σ falls into the stability interval I_{st} , i.e., when conditions $\sigma|\lambda_2| > \nu_1$ and $\sigma|\lambda_N| < \nu_2$ take place simultaneously. The equations describing the node element evolution and boundary conditions are determining the borders ν_1 and ν_2 of the stability interval I_{st} , while the eigenvalue distribution is solely ruled by the topology of the imposed wiring of connections.

3 Spatial master stability function

To analyze the stability state of the network described above we need to have the quantitative characteristic being similar to the largest Lyapunov exponent which is applicable to the spatially extended systems. It seems to be enticing and promising to use the averaged rate of the divergence of the initial close states for the description of the dynamics of the spatially extended systems in the same way as the maximum Lyapunov exponent is used for the systems with the small number of degrees of freedom. The attempts of using the concept of the largest Lyapunov exponent for the spatially extended system analysis are usually reduced to the calculation of the Lyapunov exponent in the traditional way. One of the possible methods is the calculation of the maximum Lyapunov exponent from the

time series obtained in one point of the extended system using technique developed for the system with the small number of degrees of freedom (Wolf A., Swift J., Swinney H.L., Vastano J., 1985). Alternatively, someone can calculate the spectrum of the Lyapunov exponents by means of Benettin algorithm (Benettin G., Galgani L., Giorgilli A., Strelcyn J.-M., 1980) using the discrete model of the extended system calculated with the help of the computer simulations. In this case some points of the space grid are selected as basis for the Lyapunov exponent to be calculated. The variables describing the system taken in these points are considered as components of vector state in the phase space.

In our paper we propose the quantitative characteristic called *spatial master stability function* to describe the extended systems. Let the considered spatially extended system be characterized by the state $\mathbf{U}(\mathbf{x}, t_0)$ in the moment of time t_0 (\mathbf{x} is the spatial coordinate vector). The distance $S(\mathbf{U}_1, \mathbf{U}_2)$ between two different states of the system may be defined as

$$S(\mathbf{U}_1, \mathbf{U}_2) = \left(\int_V \|\mathbf{U}_1(\mathbf{x}) - \mathbf{U}_2(\mathbf{x})\|^2 dV \right)^{1/2}, \quad (18)$$

where the integration is carried out on the space V of the extended system.

Let us consider the evolution of two systems with close (but different) initial conditions $\mathbf{U}^0(\mathbf{x}, t_0)$ and $\tilde{\mathbf{U}}^0(\mathbf{x}, t_0) = \mathbf{U}^0(\mathbf{x}, t_0) + \tilde{\xi}(\mathbf{x})$, where $\tilde{\xi}(\mathbf{x})$ is the random function, $S(\mathbf{U}^0, \tilde{\mathbf{U}}^0) = \epsilon$, with ϵ being vanishingly small. These two states evolve to $\mathbf{U}_1(\mathbf{x})$ and $\tilde{\mathbf{U}}_1(\mathbf{x})$ in time $t_0 + T$, respectively. The relation $S(\mathbf{U}_1, \tilde{\mathbf{U}}_1)/\epsilon$ describes the growth (decay) of the perturbation $\tilde{\xi}(\mathbf{x})$ during the time interval T .

Let us redefine the perturbed state $\tilde{\mathbf{U}}_1(\mathbf{x})$ in such a way for its deviation from the non-perturbed one $\mathbf{U}_1(\mathbf{x})$ be equal to the initial value ϵ : $\tilde{\mathbf{U}}_1^0(\mathbf{x}) = \epsilon \tilde{\mathbf{U}}_1 / S(\mathbf{U}_1, \tilde{\mathbf{U}}_1)$. Repeating this algorithm M times one can find the variation of the perturbation for M iteration

$$P_M = \prod_{k=1}^M S(\mathbf{R}_k, \tilde{\mathbf{R}}_k) / \epsilon. \quad (19)$$

The value of the spatial master stability function is given by

$$\Lambda = \frac{1}{MT} \ln P_M = \frac{1}{MT} \sum_{k=1}^M \ln \frac{S(\mathbf{R}_k, \tilde{\mathbf{R}}_k)}{\epsilon}. \quad (20)$$

SMSF (20) is positive if the small perturbation $\tilde{\xi}(\mathbf{x})$ brought into system increases with time, otherwise it is negative (the small perturbation decreases) or zero (the distance between perturbed and non-perturbed states of the system remains constant).

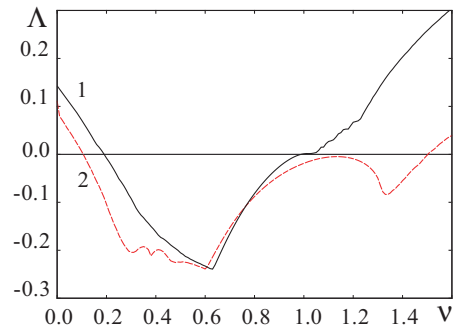


Figure 2. (Color online) The dependencies of SMSF on parameter ν for $\alpha_1 = 2.858$ (curve 1) and $\alpha_2 = 2.864$ (curve 2). In the region of the negative values of ν -parameter SMSF dependencies are positive for both the $\alpha_{1,2}$ control parameter values and all values of ν

The proposed spatial master stability function allows to describe the extended system behavior as well as the maximum Lyapunov exponent does it for the system with the small number of degrees of freedom. Obviously, it may be used both for distinguishing the chaotic and regular dynamics of extended systems and for the analyzing stability of system states (e.g., unstable periodic states in the extended system playing the role of the unstable periodic orbits embedded into chaotic attractor (Hramov A.E., Koronovskii A.A., Rempen I.S., 2006)).

Evidently, SMSF may be used to characterize the stability of the synchronous state of the network with nodes represented by the spatially extended systems like Pierce diode. The analysis of the stability of the synchronous state $[\mathbf{U}_i(x, t) = \mathbf{U}_s(x, t), \forall i]$ of network described in Sec. 2 will be given below.

4 Numerical results

In this section we consider the numerical results concerning the dynamics of the network of Pierce diodes. We consider two parameter values of node element, i.e. $\alpha_1 = 2.858$ and $\alpha_2 = 2.864$ corresponding to different regimes of chaotic behavior of Pierce diode (Filatov R.A., Hramov A.A., Koronovskii A.A., 2006). The dependencies of SMSF on the parameter ν are shown in Fig. 2 for two selected values of Pierce parameter α . Based on these dependencies one can easily predict the region of the coupling strength values where the complex network of Pierce diodes (with different topology of links between nodes) demonstrates the complete synchronization regime.

Two mutually coupled Pierce diodes being the simplest network, let us start our analysis from this elementary case. Evidently, such a system may be considered as the simplest network with the node elements $\mathbf{U}_{1,2}$ and the coupling matrix

$$G = \begin{pmatrix} -1 & 1 \\ 1 & -1 \end{pmatrix}. \quad (21)$$

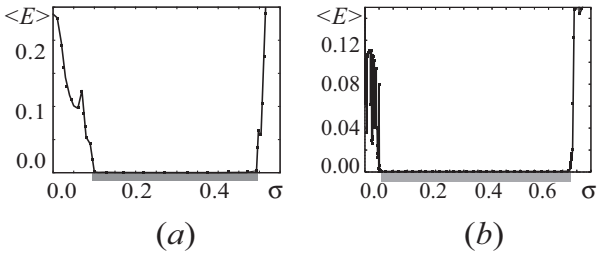


Figure 3. The synchronization error $\langle E \rangle$ (see the text of work for detail) vs the coupling strength σ for the two mutually coupled Pierce diodes with $\alpha_1 = 2.858$ (a) and $\alpha_2 = 2.864$ (b). The theoretical predictions of the synchronization regime areas based on the consideration of SMSF are shown by the gray rectangles.

It is known (see (Filatov R.A., Hramov A.A., Koronovskii A.A., 2006)) that two mutually coupled Pierce diodes show the complete synchronization regime if the coupling strength exceeds the threshold value $\sigma_c^{\alpha_1} = 0.09$ for α_1 and $\sigma_c^{\alpha_2} = 0.05$ for α_2 , respectively. It is easy to see that the eigenvalues of G are $\lambda_1 = 0$ and $\lambda_2 = -2$. Therefore, in this case the ν -parameter is equal to 2σ .

One can see from Fig. 2 that SMSF becomes negative when the condition $\nu \approx 2\sigma_c^{\alpha_1}$ is satisfied if the value of Pierce parameter is α_1 . Similarly, if the Pierce parameter value is α_2 SMSF crosses zero in the point $\nu \approx 2\sigma_c^{\alpha_2}$. In other words, two mutually coupled Pierce diodes demonstrate the complete synchronization regime when SMSF is negative. Notice, the dependence of SMSF is negative only for the values of ν -parameter belonging to the interval $(\nu_1^{\alpha_{1,2}}, \nu_2^{\alpha_{1,2}})$, $\nu_1^{\alpha_1} \approx 0.18$, $\nu_2^{\alpha_1} \approx 0.99$, $\nu_1^{\alpha_2} \approx 0.1$, $\nu_2^{\alpha_2} \approx 1.5$. Therefore, if the coupling strength σ exceeds $\sigma_2^{\alpha_{1,2}} = \nu_2^{\alpha_{1,2}}/|\lambda_2|$, the complete synchronization regime of two mutually coupled Pierce diode is also destroyed. For the selected values of Pierce parameter $\alpha_{1,2}$ the upper boundaries of the synchronous regime are $\sigma_2^{\alpha_1} = 0.495$ and $\sigma_2^{\alpha_2} = 0.750$, respectively.

So, the numerical calculation of SMSF allows to find the region of the coupling strength values corresponding to the complete synchronization regime of two coupled Pierce diodes. Moreover, the same dependence allows also to describe the stability of the synchronous state of the network consisting of the large number of Pierce diodes.

In order to show that the spatial master stability function formalism is valid and gives the correct results, the direct numerical simulation of the Pierce diode networks with the different control parameters has been carried out. This calculations allow to find the boundaries of the stability of the synchronous regime and to compare them with the analogous ones obtained above by means of SMSF consideration.

In the direct simulations of the dynamics of coupled Pierce diodes, the appearance of a synchronous state can be monitored by looking at the vanishing of the time average (over a window T) synchronization error

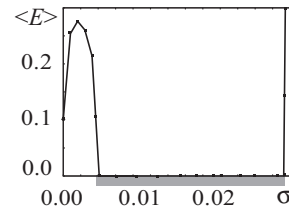


Figure 4. The synchronization error $\langle E \rangle$ vs the coupling strength σ for the network consisting of 70 coupled Pierce diodes with Pierce parameter $\alpha_2 = 2.864$. The theoretical predictions of the synchronization regime area based on the consideration of SMSF is shown by the gray rectangle.

error $\langle E \rangle$, as well as in the case of the complex network with the node elements characterized by the small number of degrees of freedom (Hwang D.-U., Chavez M., Amann A., Boccaletti S., 2005),

$$\langle E \rangle = \frac{1}{T(N-1)} \sum_{j>1} \int_t^{t+T} e_{j,1}(t') dt'. \quad (22)$$

Here $e_{i,j}(t) = \int_0^1 (|\varphi_i - \varphi_j| + |\rho_i - \rho_j| + |v_i - v_j|) dx$ is the instantaneous spatially averaged synchronization error between states $U_{i,j}(x, t)$ of two coupled Pierce diodes placed in the network nodes with numbers i and j , respectively.

Obviously, for two coupled Pierce diodes the synchronization error (22) may be rewritten as

$$\langle E \rangle = \frac{1}{T} \int_t^{t+T} e_{2,1}(t') dt'. \quad (23)$$

The synchronization errors $\langle E \rangle$ obtained for two unidirectionally coupled Pierce diodes are shown in Fig. 3, a, b. One can see that the coupling strength values $\sigma_{1,2}^{\alpha_{1,2}}$ corresponding to the destruction of the complete synchronization regime are in the excellent agreement with the theoretical predictions obtained by means of SMSF consideration for both values of the Pierce parameter $\alpha_{1,2}$.

We have also considered the complex network consisting of 70 Pierce diodes with the random symmetric zero row sum coupling matrix G . Since the distinction in the Pierce parameter values α_1 and α_2 does not cause the qualitative difference in the SMSF dependence on the ν -parameter (see Fig. 2), only one dependence of the synchronization error $\langle E \rangle$ on the coupling strength σ (for the value $\alpha_2 = 2.864$) is given in this work in Fig. 4. The minimal non-zero eigenvalue of the coupling matrix G is $\lambda_{70} = -46.06$, the maximal one — $\lambda_2 = -24.42$. The synchronous regime for such a network should be observed in the range of the coupling strength values $\sigma \in (0.0041; 0.0326)$. The synchronization error for this complex network is shown in

Fig. 4, the coupling strength value range $\sigma \in (\sigma_1; \sigma_2)$ $\sigma_1 = 0.0043$ and $\sigma_2 = 0.0325$ where the complete synchronization regime takes place being shown by the gray rectangle.

Evidently, the remarkable consistency between boundaries of synchronization obtained by means of the SMSF consideration and direct numerical calculations of the network dynamics is also observed as well as in the case of two mutually coupled Pierce diodes described above.

In conclusion, we have considered the synchronization processes in the complex networks of spatially extended chaotic systems. The technique both for the stability analysis of the synchronous state in such systems and for the spatial master stability function calculation has been developed. The efficiency of the proposed approach has been illustrated by the consideration of the complex network of Pierce diodes.

Acknowledgements

This work has been supported by RFBR (projects 08-02-90002-Bel-a and 07-02-00044) and the Supporting program of leading Russian scientific schools (project NSh-355.2008.2) and Doctor of Science (project MD-1884.2007.2). We thank also “Dynasty” Foundation.

References

Abarbanel H.D.I., Rulkov N.F., Sushchik M.M. (1996). Generalized synchronization of chaos: The auxiliary system approach. *Phys. Rev. E* **53**(5), 4528–4535.

Albert R., Barabási A.L. (2002). *Rev. Mod. Phys.*

Belykh I., Belykh V., Hasler M. (2004). Blinking model and synchronization in small-world networks with a time-varying coupling. *Physica D* **195**(1–2), 188–206.

Benettin G., Galgani L., Giorgilli A., Strelcyn J.-M. (1980). Lyapunov characteristic exponents for smooth dynamical systems and for hamiltonian systems: A method for computing all of them. p. i. theory. p. ii. numerical application. *Meccanica* **15**, 9–30.

Bezruchko B.P., Kuznetsov S.P., Trubetskov D.I. (1979). *JETP Lett.* **29**, 162.

Boccaletti S., Kurths J., Osipov G., Valladares D.L., Zhou C.S. (2002). The synchronization of chaotic systems. *Physics Reports* **366**, 1–101.

Boccaletti S., Latora V., Moreno V., Chavez M., Hwang D.-U. (2006). Complex networks: Structure and dynamics. *Physics Reports* **424**, 175–308.

Chavez M., Hwang D.-U., Amann A., Hentschel H.G.E., Boccaletti S. (2005). Synchronization is enhanced in weighted complex networks. *Phys. Rev. Lett.* **94**, 218701.

Ditto W. L., Spano M. L. et al. (1995). *Physica D* **86**(1–2), 198–211.

Dorogovtsev S.N., Mendes J.F.F. (2003). *Evolution of networks*. Oxford University Press.

Felch K.L., Danly B.G., Jory H.R. et al (1999). Char-

acteristics and applications of fast-wave gyrodevices. *Proceedings IEEE* **87**(5), 752.

Filatov R.A., Hramov A.A., Koronovskii A.A. (2006). Chaotic synchronization in coupled spatially extended beam-plasma systems. *Phys. Lett. A* **358**, 301–308.

Friedel H., Grauer R., Spatschek H.K. (1998). Controlling chaotic states of a Pierce diode. *Physics of plasmas* **5**(9), 3187–3194.

Ginzburg N.S., Kuznetsov S.P., Fedoseeva T.N. (1979). *Radiophys. Quantum Electron* **21**, 728.

Godfrey B.B. (1987). Oscillatory nonlinear electron flow in Pierce diode. *Phys. Fluids* **30**, 1553.

Hramov A.E., Koronovskii A.A. (2004). An approach to chaotic synchronization. *Chaos* **14**(3), 603–610.

Hramov A.E., Koronovskii A.A. (2005a). Generalized synchronization: a modified system approach. *Phys. Rev. E* **71**(6), 067201.

Hramov A.E., Koronovskii A.A. (2005b). Time scale synchronization of chaotic oscillators. *Physica D* **206**(3–4), 252–264.

Hramov A.E., Koronovskii A.A., Popov P.V. (2005). Generalized synchronization in coupled ginzburg-landau equations and mechanisms of its arising. *Phys. Rev. E* **72**(3), 037201.

Hramov A.E., Koronovskii A.A., Popov P.V., Rempen I.S. (2005). Chaotic synchronization of coupled electron-wave systems with backward waves. *Chaos* **15**(1), 013705.

Hramov A.E., Koronovskii A.A., Rempen I.S. (2006). Controlling chaos in spatially extended beam-plasma system by the continuous delayed feedback. *Chaos* **16**(1), 013123.

Hramov A.E., Rempen I.S. (2004). Investigation of the complex dynamics and regime control in Pierce diode with the delay feedback. *Int. J. Electronics* **91**(1), 1–12.

Hur M.S., Lee H.J., Lee J.K. (1998). Parametrization of nonlinear and chaotic oscillations in driven beam-plasma diodes. *Phys. Rev. E* **58**(1), 936–941.

Hwang D.-U., Chavez M., Amann A., Boccaletti S. (2005). Synchronization in complex networks with age ordering. *Phys. Rev. Lett.* **94**, 138701.

Ito H., Mosekilde E. et al. (1993). *Trans. Inst. Elect. Eng. Jpn. A* **113-A**(5), 365–371.

Klinger T., Latten A., Piel A., Bonhomme E., Pierre T. (1997). Chaos and turbulence studies in low- β plasmas. *Plasma Phys. Control. Fusion* **39**, B145.

Klinger T., Schroder C., Block D., Greiner F., Piel A., Bonhomme G., Naulin V. (2001). Chaos control and taming of turbulence in plasma devices. *Phys. Plasmas* **8**(5), 1961–1968.

Kolinsky, Heidrun and Hans Schamel (1995). Counterstreaming electrons and ions in pierce-like diodes. *Phys. Rev. E* **52**(4), 4267–4280.

Kuhn S., Ender A. (1990). Oscillatory nonlinear flow and coherent structures in Pierce-type diodes. *J. Appl. Phys.* **68**, 732.

Levush B., Antonsen T.M., Bromborsky A., Lou W.R., Carmel Y. (1992). Theory of relativistic backward

- wave oscillator with end reflections. *IEEE Trans. Plasma Sci.* **20**(3), 263.
- Lindsay P.A., Chen X., Xu M. (1995). Plasma-electromagnetic field interaction and chaos. *Int. J. Electronics* **79**, 237.
- Matsumoto H., Yokoyama H., Summers D. (1996). Computer simulations of the chaotic dynamics of the Pierce beam-plasma system. *Phys. Plasmas* **3**(1), 177.
- Meadows B.K., Heath T.H. et al. (2002). *Proceedings of the IEEE* **90**(5), 882.
- Motter A.E., Zhou C., Kurths J. (2005). Network synchronization, diffusion, and the paradox of heterogeneity. *Phys. Rev. E* **71**(1), 016116.
- Motter A.E., Zhou C.S., Kurths J. (2005). Enhancing complex-network synchronization. *Europhysics Letters* **69**(3), 334–340.
- Nusinovich G.S., Vlasov A.N., Antonsen T.M. (2001). Nonstationary phenomena in tapered gyro-backward-wave oscillators. *Phys.Rev.Lett.* **87**(21), 218301.
- Pecora L.M., Carroll T.L. (1990). Synchronisation in chaotic systems. *Phys. Rev. Lett.* **64**(8), 821–824.
- Pecora L.M., Carroll T.L. (1991). Driving systems with chaotic signals. *Phys. Rev. A* **44**(4), 2374–2383.
- Pecora L.M., Carroll T.L. (1998). Master stability functions for synchronized coupled systems. *Phys. Rev. Lett.* **80**(10), 2109–2112.
- Pierce J.R. (1944). Limiting currents in electron beam in presence ions. *J. Appl. Phys.* **15**, 721.
- Rosenblum M.G., Pikovsky A.S., Kurths J. (1997). From phase to lag synchronization in coupled chaotic oscillators. *Phys. Rev. Lett.* **78**(22), 4193–4196.
- Rulkov N.F., Sushchik M.M., Tsimring L.S., Abarbanel H.D.I. (1995). Generalized synchronization of chaos in directionally coupled chaotic systems. *Phys. Rev. E* **51**(2), 980–994.
- Shigaev A.M., Dmitriev B.S., Zharkov Yu.D.; Ryskin N.M. (2005). Chaotic dynamics of delayed feedback klystron oscillator and its control by external signal. *IEEE Transactions on Electron Devices* **52**(5), 790–797.
- Taherion S., Lai Y.C. (1999). Observability of lag synchronization of coupled chaotic oscillators. *Phys. Rev. E* **59**(6), R6247–R6250.
- Trubetskov A.E., Hramov A.E. (2003). *Lectures on microwave electronics for physicists (In Russian)*. Vol. 1. Fizmatlit, Moscow.
- Watts D. J., Strogatz S. (1998). *Nature (London)*.
- Watts D.J. (1999). *Small Worlds: The Dynamics of Networks between Order and Randomness*. Princeton University Press, Princeton.
- Wolf A., Swift J., Swinney H.L., Vastano J. (1985). Determining lyapunov exponents from a time series. *Physica D* **34**(6), 4971–4979.
- Zhou C., Motter A.E., Kurths J (2006). Universality in the synchronization of weighted random networks. *Phys. Rev. Lett.* **96**(3), 034101.